IEEE Photonics Journal
An IEEE Photonics Society Publication

Open Access

All-Optical Continuously Tunable Flat-Passband Microwave Photonic Notch Filter

Volume 7, Number 1, February 2015

X. Wang
J. Yang
E. H. W. Chan
X. Feng
B. Guan

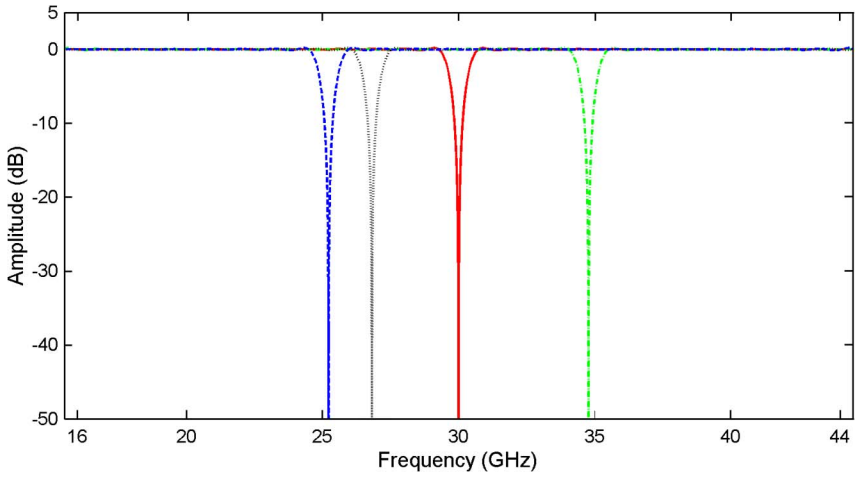

DOI: 10.1109/JPHOT.2015.2396119
1943-0655

IEEE photonics SOCIETY

IEEE

All-Optical Continuously Tunable Flat-Passband Microwave Photonic Notch Filter

X. Wang,[1] J. Yang,[1] E. H. W. Chan,[2] X. Feng,[1] and B. Guan[1]

[1]Institute of Photonics Technology, Jinan University, Guangzhou 510632, China
[2]School of Engineering and Information Technology, Charles Darwin University, Darwin, NT 0909, Australia

DOI: 10.1109/JPHOT.2015.2396119

Manuscript received December 18, 2014; revised January 19, 2015; accepted January 21, 2015. Date of publication January 26, 2015; date of current version February 11, 2015. This work was supported in part by the Natural Science Foundaton of China under Grant 61475065, by the Natural Science Foundation of Guangdong Province of China under Grant S2012010008850, and by the Fundamental Research Funds for the Central Universities in China under Grant 21612201. Corresponding author: X. Feng (e-mail: eexhfeng@ gmail.com).

Abstract: A new all-optical microwave photonic notch filter (MPNF) is presented. It is based on controlling the amplitude and phase of the optical carriers and RF phase modulation sidebands via a diffraction-based Fourier-domain optical processor. It has the ability of realizing a flat-passband, narrow-notch, and large-free-spectral-range amplitude response and a group delay response with very few ripples. The carrier and sideband optical phase controls enable a continuous notch frequency tuning operation to be realized without altering the response shape. The filter has a simple structure and a wide bandwidth as it only involves optical components. Experimental results demonstrate an MPNF that exhibits a flat passband with < 1 dB ripples, a deep notch of > 35 dB, and low group delay ripples of $< \pm 25$ ps, together with the continuous notch frequency tunability and excellent long-term stability and repeatability.

Index Terms: Microwave filter, microwave photonics, notch filter, optical signal processing.

1. Introduction

Microwave photonic signal processing has attracted significant interest in diverse areas including communications, radars, sensors, instrumentations, and so on due to the prospect of realizing extremely high multigigahertz sampling frequencies and overcoming inherent electronic bottlenecks for processing wide bandwidth signals [1]. It also has the supplementary advantages of reconfigurability and immunity to electromagnetic interference.

Microwave photonic notch filters (MPNFs) have applications, such as distributed fiber-fed antennas in defense systems [2], where specific RF/microwave frequency components need to be eliminated. To avoid attenuation on other frequency components around the desired null, MPNFs are required to have a flat passband and a narrow notch width frequency response. Many MPNFs implemented using various techniques have been reported [3]–[13]. Infinite impulse response (IIR) structure based MPNFs [3] can realize a high resolution filter response but have limited free spectral range (FSR), which reduces the filter operating frequency range. Furthermore the notch frequency cannot be tuned continuously. The technique presented in [4] solves the

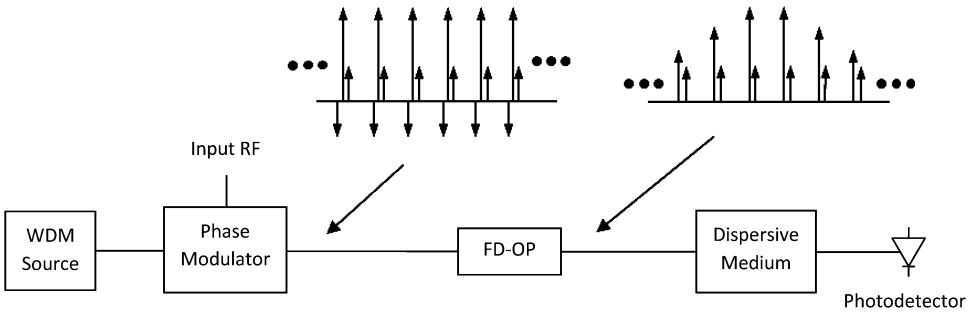

Fig. 1. Topology of the novel all-optical MPNF and the optical spectrums before and after the FD-OP.

limited FSR and continuous notch frequency tuning problems, but the filter passband is not flat, and the passband amplitude changes when tuning the notch frequency. The stimulated Brillouin scattering (SBS) based MPNFs [5], [6] can realize a large-FSR continuously-tunable notch filter response. However, the SBS-based microwave photonic filters suffer from a high SBS noise because SBS is an amplification process which adds noise to the signal [14]. It also has the long-term stability problem due to the signal polarization dependent frequency response. Moreover, they have a complex structure as two or more electro-optic modulators are needed. Furthermore, a recent study found that the frequency response of an SBS based microwave photonic filter is dependent on the input RF signal power. A technique has been proposed to ease the input RF signal power dependent frequency response problem, but the problem remains unsolved [15]. Approaches based on finite impulse response (FIR) structures have a robust frequency response that is independent of changes in environmental condition and is also independent of the input RF signal power. However, most previously reported FIR structure based MPNFs have been limited to only two taps [7]–[9], or to just four taps [10]–[12], which produce a response that is much too gradual, causing significant frequency-dependent attenuation in the required passband that can corrupt the wanted information signal itself. A technique has been proposed to realize a multiple-tap MPNF [13]. However, the problem of group delay ripples arises due to unequal tap separation, and the notch frequency cannot tune continuously. Until now there is no report on a continuously-tunable, flat-passband MPNF with low group delay ripples and robust frequency response performance.

In this paper, we present a new all-optical continuously-tunable MPNF that can simultaneously realize a flat passband and a large FSR notch filter response with low group delay ripples. It is based on controlling the amplitude and phase of the optical carrier and RF phase modulation sidebands via a diffraction-based Fourier-domain optical processor (FD-OP). This enables the synthesis of the required sinc function distribution impulse response having equally-separated taps with the desired phase for the notch frequency tuning operation. The filter only involves optical components and has a single-optical-source, single-modulator and single-photodetecotor structure. Experimental results are presented that demonstrate a large FSR and flat passband notch filter response with low group delay ripples. The notch filter long term stability and repeatability measurement are also presented. Continuous notch frequency tuning operation is experimentally demonstrated.

2. Topology and Principle of Operation

The topology of the novel all-optical MPNF is shown in Fig. 1. The light from a wavelength division multiplexing (WDM) source is phase modulated by an input RF signal and is launched into a FD-OP. The FD-OP is based on a two-dimensional liquid crystal on silicon (LCoS) pixel array, which can distribute the phase modulated signals to different locations on the LCoS array dependent on the wavelengths of the WDM source [16]. The FD-OP has two functions in this MPNF. One is that it filters out one sideband of the phase modulated signal to realize single sideband (SSB) modulation to avoid the dispersion induced power fading problem [17]; another

is that it controls the amplitude and phase of the carrier and the remaining sideband independently for each wavelength of the WDM source. This is done by programming the horizontal and vertical axis of the LCoS pixel panel. The multiple-wavelength Fourier-domain optical processed signals then pass through a dispersive medium to introduce delays between different wavelengths and are detected by a photodetector.

Each wavelength from the WDM source can generate one delayed optical signal or tap formed by the beating between the carrier and the corresponding sideband at the photodetector. The tap amplitude is proportional to the product of the carrier and the sideband amplitude. The phase shift of the tap equals to the phase difference between the carrier and the corresponding sideband. A flat passband notch filter response can be obtained by programming the FD-OP such that the taps have a sinc function distribution in the filter impulse response. The resolution of the notch filter is dependent on the number of taps, which in turn depends on the number of wavelengths generated by the WDM source. Various techniques such as spectrum slicing a broadband optical source or multiwavelength erbium-doped fiber laser, which is capable of generating 50 wavelengths [18], can be used to generate many wavelengths to realize a high resolution notch filter response. Since the tap separation is proportional to the wavelength separation and the dispersion parameter of the dispersive medium, which can be made to be small, the structure has the ability to realize a large FSR frequency response. It should be noted that the ability to independently control the amplitude and the phase shift of each tap enables a highly reconfigurable notch filtering operation to be realized.

3. Analysis and Design

Assuming a WDM source with N wavelengths is used in the novel all-optical MPNF. The electric field at the output of the phase modulator can be expressed as

$$E(t)=\sum_{n=1}^{N}E_{\text{in},n}\sqrt{t_{ff}}\left[J_0(\beta_{\text{RF}})\exp j(\omega_{c,n}t)-J_1(\beta_{\text{RF}})\exp j(\omega_{c,n}-\omega_{\text{RF}})t+J_1(\beta_{\text{RF}})\exp j(\omega_{c,n}+\omega_{\text{RF}})t\right] \quad (1)$$

where n is the wavelength index, $E_{\text{in},n}$ is the amplitude of the electric field of the nth wavelength at the input of the phase modulator, t_{ff} is the phase modulator insertion loss, $J_m(x)$ is the Bessel function of mth order of first kind, $\beta_{\text{RF}}=\pi V_{\text{RF}}/V_{\pi}$ is the modulation index, V_{RF} is the modulator input RF signal amplitude, V_{π} is the switching voltage of the optical phase modulator, and $\omega_{c,n}$ and ω_{RF} are the nth wavelength optical carrier and input RF signal angular frequency, respectively. The FD-OP is programmed to remove the lower sideband of the RF phase modulated optical signal, to introduce a phase shift to the carrier and the upper sideband, and to control the carrier and the upper sideband amplitude, as was discussed in the previous section. The electric field at the FD-OP output can be expressed as

$$E(t)=\sum_{n=1}^{N}E_{\text{in},n}\sqrt{t_{ff}}\left[\sqrt{\alpha_{c,n}}J_0(\beta_{\text{RF}})\exp j(\omega_{c,n}t+\phi_{c,n})+\sqrt{\alpha_{s,n}}J_1(\beta_{\text{RF}})\exp j\big((\omega_{c,n}+\omega_{\text{RF}})t+\phi_{s,n}\big)\right] \quad (2)$$

where $\alpha_{c,n},\alpha_{s,n}$ are the power attenuation of the nth wavelength carrier and upper sideband respectively, and $\phi_{c,n},\phi_{s,n}$ are the phase shift of the nth wavelength carrier and upper sideband respectively. The dispersive medium introduces time delay to the different wavelength carriers and the upper sidebands. Since the separations of all the wavelengths of the WDM source are equal, the electric field after the dispersive medium can be expressed as

$$E(t)=\sum_{n=1}^{N}E_{\text{in},n}\sqrt{t_{ff}}\left[\sqrt{\alpha_{c,n}}J_0(\beta_{\text{RF}})\exp j\big(\omega_{c,n}(t+(n-1)\tau)+\phi_{c,n}\big)\right.$$
$$\left.+\sqrt{\alpha_{s,n}}J_1(\beta_{\text{RF}})\exp j\big((\omega_{c,n}+\omega_{\text{RF}})(t+(n-1)\tau)+\phi_{s,n}\big)\right]. \quad (3)$$

We assume the separation of the WDM source wavelength is wide enough so that the photodetector only detects the beating of the carrier and its sideband. The optical power at the RF

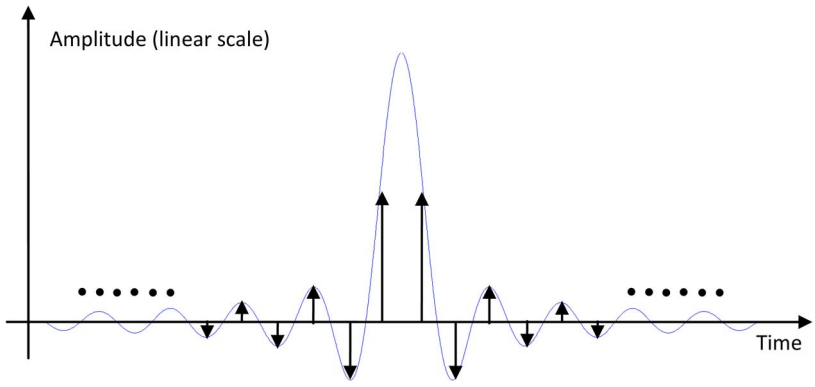

Fig. 2. Impulse response of the novel all-optical MPNF.

frequency into the photodetector, which is the electric field square, is given by

$$P_{\text{out}} = 2t_{ff}J_0(\beta_{\text{RF}})J_1(\beta_{\text{RF}})\sqrt{A^2+B^2} \tag{4}$$

where

$$A = \sum_{n=1}^{N} P_{\text{in},n}\sqrt{\alpha_{c,n}}\sqrt{\alpha_{s,n}}\cos\left[\omega_{\text{RF}}(n-1)\tau + \Delta\phi_n\right] \tag{5}$$

$$B = \sum_{n=1}^{N} P_{\text{in},n}\sqrt{\alpha_{c,n}}\sqrt{\alpha_{s,n}}\sin\left[\omega_{\text{RF}}(n-1)\tau + \Delta\phi_n\right] \tag{6}$$

where $P_{\text{in},n}$ is the optical power of the nth wavelength from the WDM source, $\tau = \Delta\lambda D$ is the basic time delay, $\Delta\lambda$ is the wavelength separation, D is the dispersion parameter of the dispersive medium with a unit of ps/nm, and $\Delta\phi_n = \phi_{s,n} - \phi_{c,n}$. Under the small signal condition, the filter transfer function, which is defined as the ratio of the output and input RF signal power, can be obtained from (4) and can be written as

$$|H(f_{\text{RF}})|^2 = \left(\frac{\pi}{V_\pi}\right)^2 R_{\text{in}}R_o t_{ff}^2\Re^2(A^2+B^2) \tag{7}$$

where $\Re$ is the photodiode responsivity, R_{in} is the modulator input resistance, and R_o is the photodetector load resistance.

The above analysis shows the amplitude and phase of the nth tap are dependent on $\alpha_{c,n}\alpha_{s,n}$ and $\Delta\phi_n = \phi_{s,n} - \phi_{c,n}$ respectively. This indicates that the amplitude and phase of each tap can be controlled independently by programming the FD-OP. In order to obtain a notch filter response with a wide and flat passband, the tap amplitudes in the impulse response are designed to have a sinc function distribution, as illustrated in Fig. 2. It can be seen from the figure that the tap distribution is symmetrical. The middle two taps have the largest and equal amplitudes, and the same phase of 0°. The next pair of taps has a 180° phase difference relative to the middle two taps. By extending the number of taps in pair with this sinc function distribution, the notch filter resolution can be increased. The simulated notch filter frequency responses for two, four, six, eight and thirty-two taps with $\tau = 0.05$ ns, which correspond to a FSR of 20 GHz, are shown in Fig. 3. It can be seen that the operating frequency range of the 32-tap MPNF is around 40 GHz. The filter passband is flat with 0.4 dB ripples. The -6 dB notch width over the -3 dB operating range of the notch filter is improved from 22.3% to 1.3% when the number of taps is increased from 2 to 32. The notch width can be narrowed by using more taps. Note that while the number of taps increases, the passband ripple amplitude can always be kept $<$ 0.4 dB. It should be pointed out that a wavelength-independent dispersion parameter D was used in the simulation. A normal single mode fiber has around 2.5 ps/nm $\cdot$ km changes in the dispersion values for 50 nm

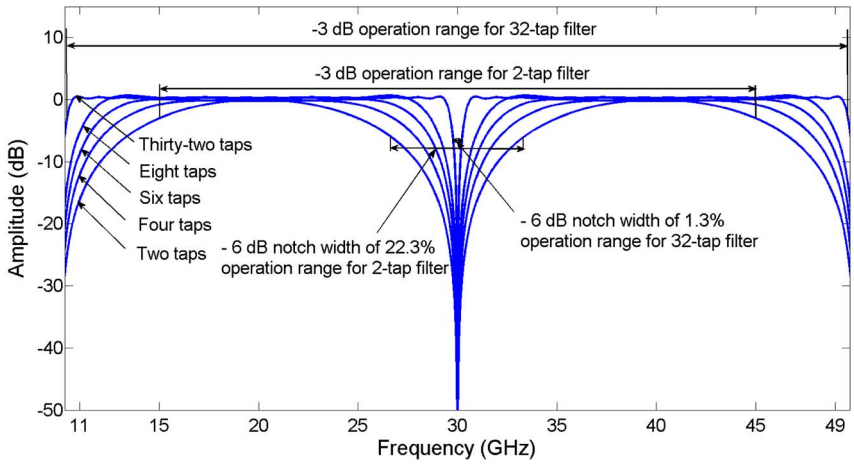

Fig. 3. Simulated frequency response for two, four, six, eight, and 32 taps notch filter.

changes in the wavelength. With the inclusion of this wavelength dependent effect in the simulation, the 32-tap notch filter response has ∼2 dB ripples at around the 30 GHz notch frequency and the filter notch width is slightly increased. Fortunately, the group delay ripple compensation function in the commercial FD-OP [19] can be used to overcome the unwanted effect caused by the wavelength-dependent dispersion characteristic in the normal single mode fiber. Alternatively, a photonic crystal fiber with a flat dispersion characteristic [20] can be used as the dispersion medium in the notch filter structure.

Thanks to the optical phase control function in the FD-OP, the notch frequency can be continuously tuned by designing the phase shift of the *n*th tap to be

$$\Delta\phi_n = \Delta\phi'_n + n\theta \tag{8}$$

where $\Delta\phi'_n$ is the original phase shift of the *n*th tap and is either 0° or 180°, as shown in Fig. 2, and $n\theta$ is the extra phase required to be added to the *n*th tap for tuning the notch frequency. The notch frequency is given by

$$f_{\text{notch}} = f'_{\text{notch}} + \frac{\theta}{2\pi\Delta\lambda D} \tag{9}$$

where f'_{notch} is the original *k*th harmonic notch frequency and is given by

$$f'_{\text{notch}} = \frac{2k-1}{2\Delta\lambda D}. \tag{10}$$

This shows the filter notch frequency is dependent on the dispersion parameter of the dispersive medium D and θ which can be controlled using the FD-OP. For illustration of the notch frequency tuning operation, the notch frequency is tuned from 25.2 GHz to 34.8 GHz by using different values of θ, as shown in Fig. 4. It can be seen from the figure that by changing the θ values from 0 to -1.5, -1, and 1.5 rad, the notch frequency is tuned from 30 GHz to 25.2 GHz, 26.8 GHz, and 34.8 GHz respectively. Since θ can be any value between $-\pi$ to π rad by controlling $\Delta\phi = \phi_s - \omega_c$, the filter notch frequency can be continuously tuned over the full FSR range. Note that while tuning the notch frequency, the notch width and the FSR of the notch filter remain unchanged. This shows the advantage of the novel optical phase control notch frequency tuning technique compared to the conventional technique that uses a wavelength tunable laser and a wavelength dependent time delay element to change the fundamental time delay of the structure, which alters not only the notch frequency but also the response shape.

The novel all-optical MPNF has a simple structure. It only requires a single WDM source, a single optical phase modulator, a programmable FD-OP, a dispersive medium, and a single

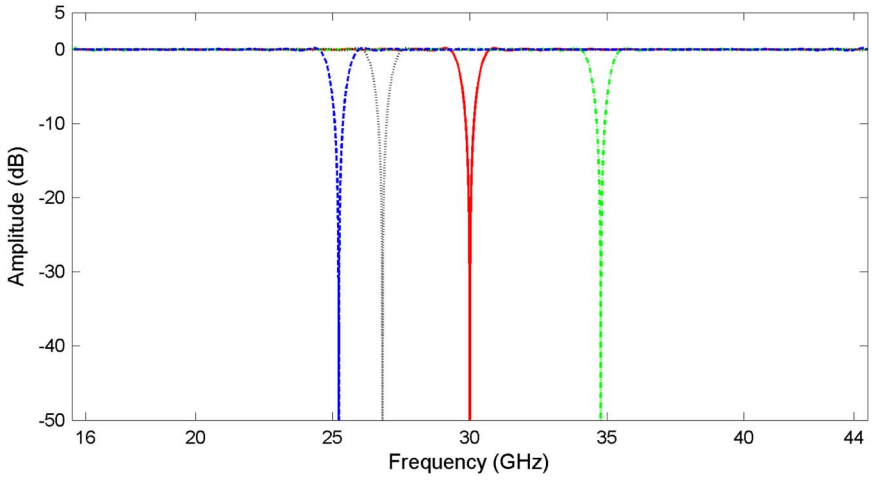

Fig. 4. Simulated tunable notch filter frequency response for $\theta = -1.5$ rad (dashed line), -1 rad (dotted line), 0 rad (solid line), and 1.5 rad (dot-dash line).

photodetector, which are commercially available [21]. Since no electrical components are involved in the structure, this MPNF can be operated in microwave and even millimeter wave frequency range. The bandwidth of this MPNF is only limited by the optical modulator bandwidth. Since only a normal electro-optic phase modulator is needed and an electro-optic modulator with 100 GHz bandwidth has been reported [22], the notch filter can operate to at least 100 GHz. Using an optical phase modulator has the advantage of no DC bias voltage required and no bias drift problem, which is presented in the conventional fiber optic links that use an optical intensity modulator for RF signal modulation. It should be noted that all the tap separations are equal. This enables the realization of a linear phase response. Consequently the filter exhibits a constant group delay, which is significant because it does not cause signal phase distortion, especially in radar applications where the frequency content of a radar pulse needs to be treated the same over the intended bandwidth of frequencies. The notch filter does not suffer from the phase-induced intensity noise problem which generates in the conventional IIR structure based filter and the SBS noise which generates in the SBS based filter. Moreover, since each tap is generated by a different wavelength, the filter is free of coherence. Therefore it has a very robust response insensitive to environmental perturbations. In order to realize a high-resolution notch filter response with a deep notch and a flat passband, the tap amplitudes and separations need to be set to the desired values. The tap amplitudes and separations are determined by the amplitude and separation of each laser source wavelength. Hence a stable multiwavelength laser source is required for the notch filter to be operated in practice. Laser arrays with 56 wavelengths are commercially available [23]. The laser has excellent power and frequency stability of 0.03 dB and ± 0.3 GHz over 24 hr. It is suitable for use as the multiwavelength source for the notch filter to obtain a stable performance when the system is operated in practice.

4. Experimental Results

Experiments were conducted with the experimental setup as shown in Fig. 5 to verify the principle for the novel all-optical MPNF. The WDM source was a Fabry-Perot (FP) laser, which was operated at around 1550 nm and had a wavelength separation of 1.26 nm. It was followed by an optical filter that selected the eight wavelengths at the center of the FP laser spectrum. A polarization controller (PC) was used to align the FP laser light polarization state to maximize the efficiency of the phase modulator. The different-wavelength RF phase modulated optical signals were amplified by an erbium-doped fiber amplifier (EDFA) and were processed by a FD-OP (Finisar WaveShaper 4000S), which was programmed to eliminate the lower sidebands and to

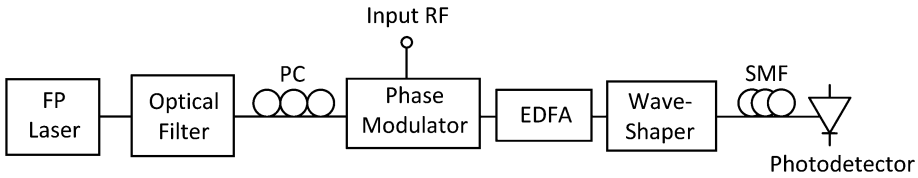

Fig. 5. Experimental setup of the novel all-optical MPNF.

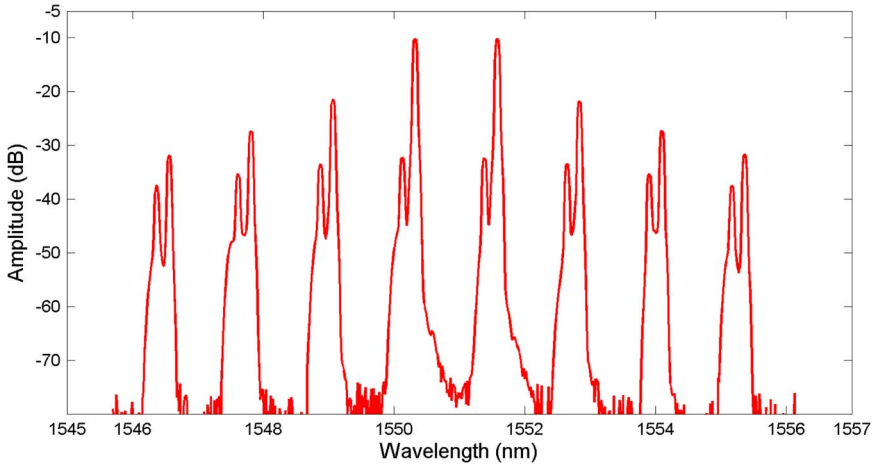

Fig. 6. Measured optical spectrum after the FD-OP for an eight-tap notch filter.

set the phase and amplitude of the different wavelength optical carriers and upper sidebands to the desired values. The resolution of the FD-OP used in the experiment was 12 GHz. The optical spectrum after the FD-OP was measured using an optical spectrum analyzer and is shown in Fig. 6. The measurement was obtained when the phase modulator was driven by a 23 GHz frequency RF signal and eight wavelengths from the FP laser were used as the source. It can be seen from the figure that the right sideband in the optical domain for each wavelength are filtered out by the FD-OP. The figure shows the amplitude of the carrier and the right sideband for each wavelength were programmed by the FD-OP to obtain the sinc function distribution impulse response as was discussed in the previous section. The processed signal passed through a length of 20 km single mode fiber (SMF) with a dispersion parameter of 17 ps/km $\cdot$ nm and was detected by a 50 GHz bandwidth photodetector connected to a 26.5 GHz bandwidth network analyzer to display the filter frequency response. The FD-OP was programmed to generate a notch filter with two, four, six and eight taps, and the corresponding frequency responses were measured as shown in Fig. 7.

The filter FSR was 2.33 GHz determined by the length of the 20 km long fiber, which generated a basic time delay of 0.43 ns. The highest measurement frequency of 26.5 GHz was limited by the bandwidth of the network analyzer. Excellent agreement between the experimental and simulated results can be seen in Fig. 7. The filter -6 dB notch width is narrowed from 21.9% to 5.1% of the -3 dB operating frequency range, as the number of taps is increased from 2 to 8. The measured amplitude ripple in the notch filter passband was <1 dB. This demonstrates that the novel all-optical MPNF structure has the ability to realize a notch filter response with a narrow notch width and a flat passband. The measured notch depth was over 40 dB, and the filter response was stable. The stability of the novel all-optical MPNF was investigated by measuring the eight-tap notch filter frequency response for 8 hr. The eight-tap notch filter frequency response was recorded in every 15 min and is shown in Fig. 8(a).

It can be seen from Fig. 8(a) that the notch filter frequency response is stable for a long period of time. The notch depth was more than 35 dB throughout the 8-hr period. The notch filter

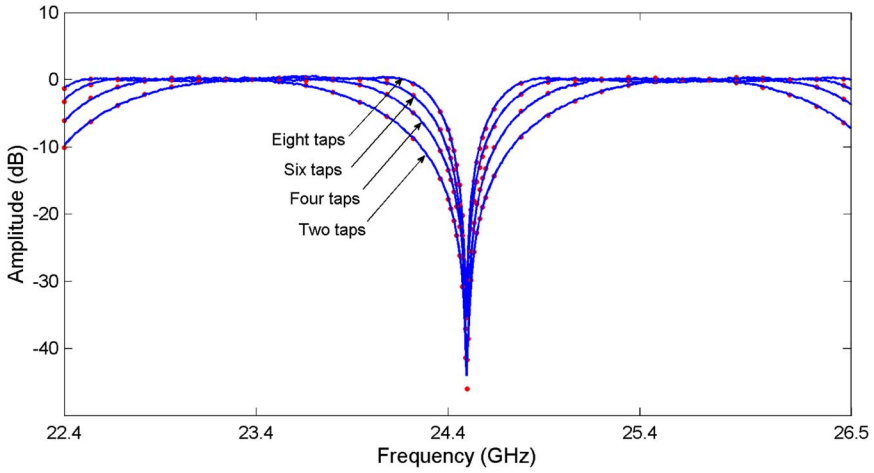

Fig. 7. Simulated (dotted lines) and measured (solid lines) frequency responses with two, four, six, and eight taps.

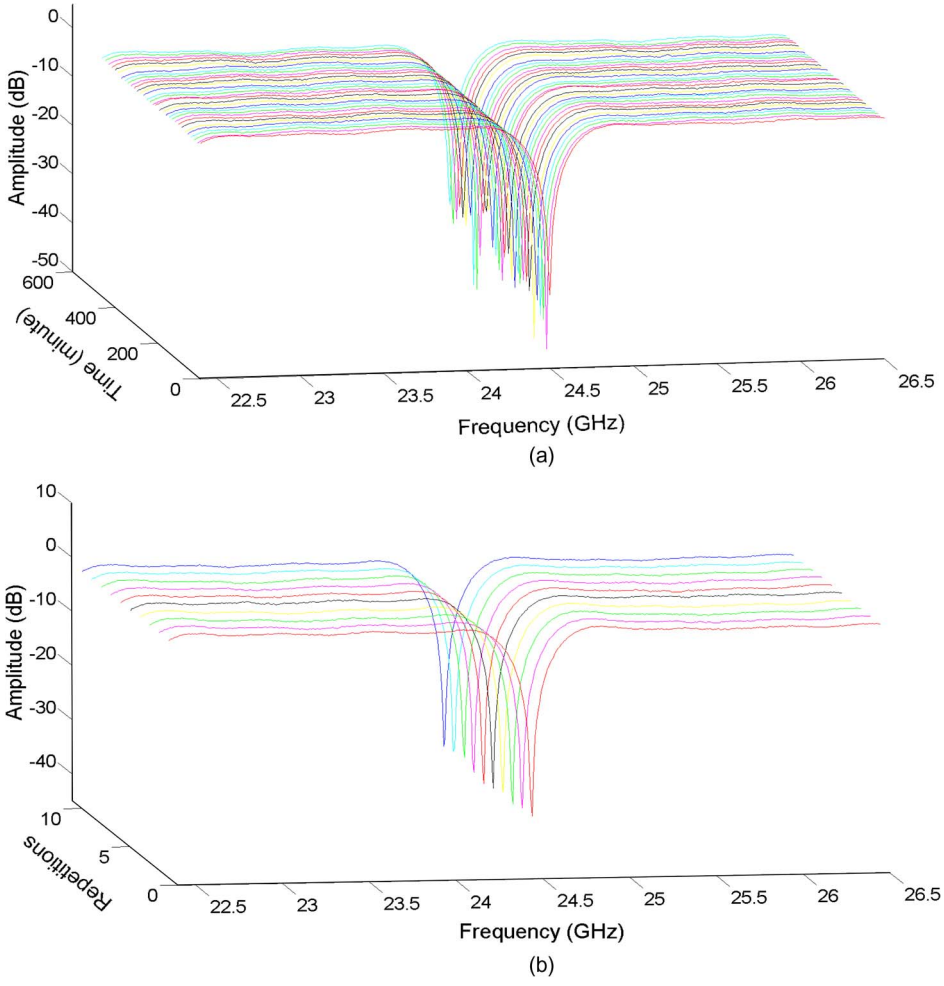

Fig. 8. Measured notch filter responses recorded (a) in every 15 min for 8 hr for the stability investigation and (b) after reloading the same program file to the FD-OP in every half hour for the repeatability investigation.

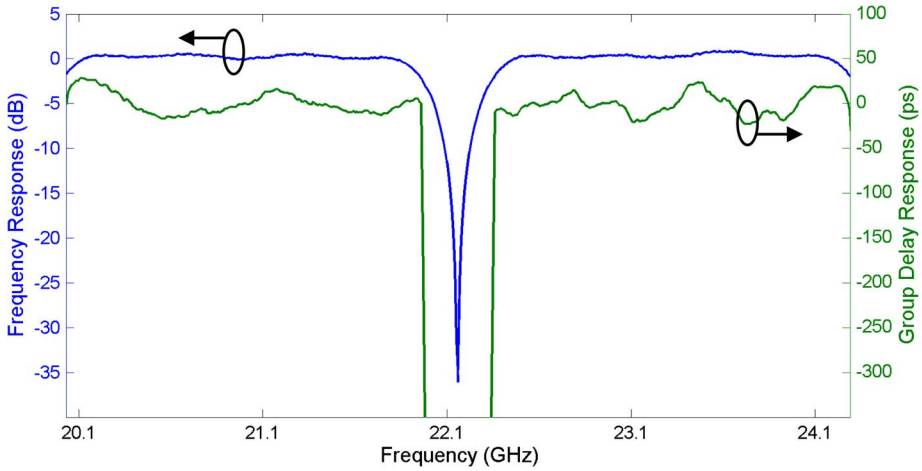

Fig. 9. Measured frequency response and group delay response within the notch filter −3 dB operating frequency range.

passband amplitude had less than 1 dB variation. With regard to repeatability, the same program file for realizing an eight-tap notch filter response was loaded to the FD-OP in every half hour 10 times, and the frequency responses were recorded as shown in Fig. 8(b). Again, the notch depth was more than 35 dB and the change in the notch filter passband amplitude was less than 1 dB. This demonstrates the novel all-optical MPNF has an excellent long term stability and repeatability performance, which cannot be achieved by many reported MPNF structures. It should be pointed out that using a shorter fiber as the dispersive medium can increase the filter frequency response FSR, and using a WDM source such as the multiwavelength erbium-doped fiber laser [18] that generates many wavelengths can increase the filter resolution.

Fig. 9 shows the measured group delay response of the novel all-optical MPNF. The group delay in the filter passband is essentially flat, with the small residual group delay variation being mainly due to a slight asymmetrical tap distribution in the filter impulse response and some measurement noise. The result shown in Fig. 9 exhibits a group delay variation and ripple of $< \pm 25$ ps in the filter passband, which can satisfy the requirements of radar applications [24], [25].

The signal-to-noise ratio (SNR) of the novel all-optical MPNF was measured to be 112 dB/Hz, which is similar to other reported MPNF SNRs [3], for an input RF signal power of 5 dBm into the phase modulator and an output optical power of 0 dBm into the photodetector. The signal-spontaneous beat noise from the EDFA and the laser intensity noise from the FP laser were found to be the dominant noise sources in the MPNF. The filter SNR can be increased by using a high-power WDM source with low relative intensity noise.

Two notch frequency tuning operations were demonstrated experimentally. First, discrete notch frequency tuning was demonstrated by changing the value of the dispersion parameter D in (9). This can be done by using different length of fiber as the dispersive medium. Fig. 10(a) shows the measured notch frequency responses when using different lengths of SMF in the MPNF structure. By changing the SMF length from 20 km to 14.35 km, the basic time delay τ was changed to 0.33 ns. This, in turn, changed the notch filter FSR from 2.33 GHz to 2.99 GHz and consequently changed the notch frequency. This technique can only provide discrete notch frequency tuning. Another technique, which enables continuous notch frequency tuning, was demonstrated by controlling the phases of different-wavelength optical carriers and sidebands according to (8) via the FD-OP while keeping the SMF length fixed at 20 km. The measured continuously tunable notch filter response is shown in Fig. 10(b). The notch frequency was tuned from 22.16 GHz to 21.84 GHz by changing the value of θ from 0 to −0.86 rad and agrees with (9). The notch depth of $>$ 35 dB was maintained while tuning the notch frequency. The −6 dB notch width as well as the FSR remained the same when the notch frequency was tuned. This shows the advantage of controlling the phase shift compared to changing the fiber

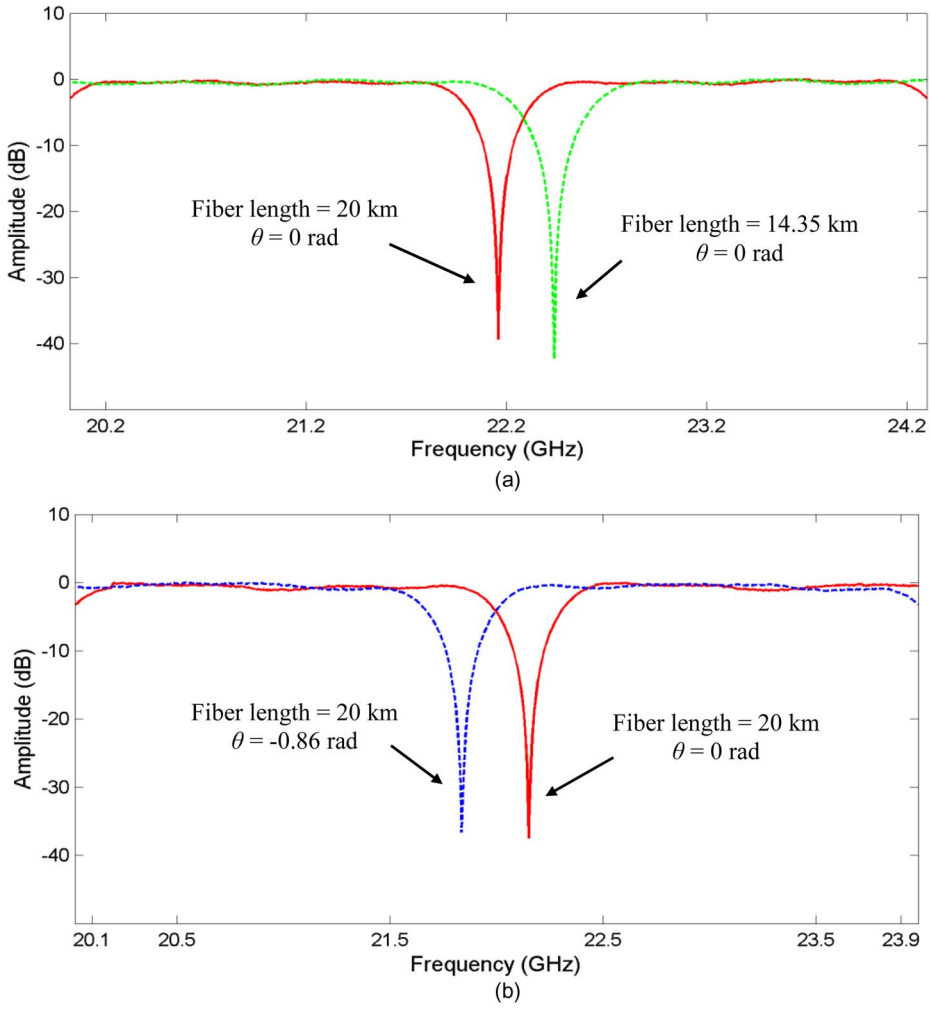

Fig. 10. Experimental results of (a) discrete and (b) continuously tunable notch filter.

length to tune the notch frequency as it not only provides continuous tuning operation without physically changing the system configuration but also does not affect the notch filter frequency response shape.

5. Conclusion

A new all-optical MPNF structure that can realize a flat and wide passband, large FSR, and flat group delay characteristic frequency response together with continuous notch frequency tuning operation has been presented. It is based on controlling the amplitude and phase of the different-wavelength delayed optical signals via a diffraction-based Fourier-domain optical processor. The novel technique is free of DC bias and the bias drift problem as an optical phase modulator is used for RF signal modulation. It has excellent frequency response stability and repeatability performance. It does not suffer the RF signal power dependent frequency response problem, which is experienced in SBS based filters. Experimental results have demonstrated a multiple-tap MPNF, exhibiting a flat passband, a deep notch of > 35 dB, and a low group delay ripple of $< \pm 25$ ps. The long term stability and repeatability performance, and continuous notch frequency tuning operation have also been demonstrated. The novel all-optical MPNF offers high-performance notch filtering to microwave and millimeter wave frequency suitable for communication, defense, and radio astronomy applications.

References

[1] R. A. Minasian, E. H. W. Chan, and X. Yi, "Microwave photonic signal processing," *Opt. Exp.*, vol. 21, no. 19, pp. 22 918–22 936, Sep. 2013.

[2] J. Capmany, B. Ortega, and D. Pastor "A tutorial on microwave photonic filters," *J. Lightw. Technol.*, vol. 24, no. 1, pp. 201–229, Jan. 2006.

[3] E. H. W. Chan and R. A. Minasian, "High-resolution tunable RF/microwave photonic notch filter with low-noise performance," *J. Lightw. Technol.*, vol. 29, no. 21, pp. 3304–3309, Nov. 2011.

[4] R. Tao, X. Feng, Y. Cao, Z. Li, and B. Guan, "Tunable microwave photonic notch filter and bandpass filter based on high-birefringence fiber-Bragg-grating-based Fabry-Perot cavity," *IEEE Photon. Technol. Lett.*, vol. 24, no. 20, pp. 1805–1808, Oct. 2012.

[5] W. Zhang and R. A. Minasian, "Ultra-wide tunable microwave photonic notch filter based on stimulated Brillouin scattering," *IEEE Photon. Technol. Lett.*, vol. 24, no. 14, pp. 1182–1184, Jul. 2012.

[6] D. Marpaung, B. Morrison, R. Pant, and B. J. Eggleton, "Frequency agile microwave photonic notch filter with anomalously high stopband rejection," *Opt. Lett.*, vol. 38, no. 21, pp. 4300–4303, Nov. 2013.

[7] W. Li, N. Zhu, and L. Wang, "Continuously tunable microwave photonic notch filter with a complex coefficient," *IEEE Photon. J.*, vol. 3, no. 3, pp. 462–467, Jun. 2011.

[8] C. Zhang *et al.*, "A tunable microwave photonic filter with a complex coefficient based on polarization modulation," *IEEE Photon. J.*, vol. 5, no. 5, Oct. 2013, Art. ID. 5501606.

[9] Y. Zhang and S. Pan, "Complex coefficient microwave photonic filter using a polarization-modulator-based phase shifter," *IEEE Photon. Technol. Lett.*, vol. 25, no. 2, pp. 187–189, Jan. 2013.

[10] E. H. W. Chan and R. A. Minasian, "Coherence-free equivalent negative tap microwave photonic notch filter based on delayed self-wavelength conversion," *IEEE Trans. Microw. Theory Tech.*, vol. 58, no. 11, pp. 3199–3205, Nov. 2010.

[11] X. Li *et al.*, "Microwave photonic filter with multiple taps based on single semiconductor optical amplifier," *Opt. Commun.*, vol. 283, no. 15, pp. 3026–3029, Aug. 2010.

[12] X. Wang, E. H. W. Chan, and R. A. Minasian, "Microwave photonic notch filter based on a dual-Sagnac-loop structure," *Appl. Opt.*, vol. 49, no. 33, pp. 6546–6551, Nov. 2010.

[13] E. H. W. Chan and R. A. Minasian, "Multiple-tap, tunable microwave photonic interference mitigation filter," *J. Lightw. Technol.*, vol. 29, no. 8, pp. 1069–1076, Apr. 2011.

[14] N. A. Olsson and J. P. Van Der Ziel, "Characteristics of a semiconductor laser pumped Brillouin amplifier with electronically controlled bandwidth," *J. Lightw. Technol.*, vol. LT-5, no. 1, pp. 147–153, Jan. 1987.

[15] M. Pagani, E. H. W. Chan, and R. A. Minasian, "A study of the linearity performance of a stimulated Brillouin scattering-based microwave photonic bandpass filter," *J. Lightw. Technol.*, vol. 32, no. 5, pp. 999–1005, Mar. 2014.

[16] M. A. F. Roelens *et al.*, "Dispersion trimming in a reconfigurable wavelength selective switch," *J. Lightw. Technol.*, vol. 26, no. 1, pp. 73–78, Jan. 2008.

[17] J. L. Corral, J. Marti, J. M. Fuster, and R. I. Laming, "Dispersion induced bandwidth limitation of variable true time delay lines based on linearly chirped fiber gratings," *Electron. Lett.*, vol. 34, no. 2, pp. 209–211, Jan. 1998.

[18] X. Feng, H. Tam, H. Liu, and P. K. A. Wai, "Multiwavelength erbium-doped fiber laser employing a nonlinear optical loop mirror," *Opt. Commun.*, vol. 268, no. 2, pp. 278–281, Dec. 2006.

[19] Finisar Application Note, "Group delay ripple compensation," 2012. [Online]. Available: http://www.finisar.com/sites/default/files/pdf/WaveShaper%20-%20Group%20Delay%20Ripple%20Compensation.pdf

[20] M. Klimczak *et al.*, "Coherent supercontinuum generation up to 2.3 μm in all-solid-glass photonic crystal fibers with flat all-normal dispersion," *Opt. Exp.*, vol. 22, no. 15, pp. 18 824–18 832, Jul. 2014.

[21] *WaveShaper 4000S Multiport Optical Processor Data Sheet*. [Online]. Available:www.finisar.com

[22] H. Huang *et al.*, "Broadband modulation performance of 100-GHz EO polymer MZMs," *IEEE Photon. Technol. Lett.*, vol. 30, no. 23, pp. 3647–3652, Dec. 2012.

[23] *ID Photonics PX Laser Source Slide-in Card and CBSL56 Mainframe*. [Online]. Available: http://www.id-photonics.com/index.php/products

[24] Y. J. Cho, K. H. Kim, D. H. Choi, S. S. Lee, and S. O. Park, "A miniature UWB planar monopole antenna with 5-GHz band-rejection filter and time-domain characteristics," *IEEE Trans. Antennas Propag.*, vol. 54, no. 5, pp. 1453–1460, May 2006.

[25] F. P. Martinez, M. B. Garcia, and A. A. Lopez, "Group delay effects on the performance of wideband CW-LFM radars," *Proc. Inst. Elect. Eng., Radar, Sonar Navigat.*, vol. 148, no. 2, pp. 95–100, Apr. 2001.